IEEJ Journal of Industry Applications
Vol.6 No.3 pp.192–198 DOI: 10.1541/ieejjia.6.192

Paper

Design of an Infinite-Order Disturbance Observer Enhancing Disturbance Suppression Performance

Hisayoshi Muramatsu* Student Member, Seiichiro Katsura* Senior Member

(Manuscript received March 8, 2016, revised Nov. 20, 2016)

This paper presents the design of an infinite-order disturbance observer (IFDOB) to suppress disturbances including a periodic disturbance. An IFDOB includes the dynamics of a periodic disturbance to suppress it. However, a conventional IFDOB finds it difficult to suppress disturbances in the low-frequency domain. In contrast, a disturbance observer (DOB) can suppress disturbances in the low-frequency domain, however, it has difficulty suppressing a periodic disturbance. Therefore, this paper proposes a designed IFDOB that can suppress both a periodic disturbance and low-frequency disturbances. The proposed method is constructed by designing parameter γ of an IFDOB considering sensitivity and complementary sensitivity functions. Simulations were conducted, and the validity of the proposed method in a practical system was confirmed by experiments using a multi-axis manipulator.

Keywords: periodic disturbance, disturbance observer, infinite-order disturbance observer, time-delay element

1. Introduction

In motion control system, robustness is necessary against disturbances to realize precise motion, because the precise motion of industrial machines improves quality of productions. Especially, for periodically working industrial machines, the robustness against an induced periodic disturbance is important in the industrial field. The periodic disturbance is a serious problem because of including harmonics in the motion control. Disturbances in the high-frequency domain such as the harmonics are difficult to suppress.

In conventional studies, control methods have been widely studied to suppress disturbances. In a linear control system, the internal model principle is utilized to eliminate a disturbance [(1)]. Both proportional-integral-derivative (PID) controller [(2)] and a disturbance observer (DOB) [(3)] are based on the internal model of a disturbance to suppress. Thus, the internal model principle is effective and clear to design a linear controller [(4)].

PID control is major control in the classical control theory. Characteristics of PID control can be arbitrarily modified by PID gains [(5)(6)]. Implementation of PID control is simple, because the PID controller can be designed without a rigorous model. However, PID control affects both performances of trajectory tracking and disturbance suppression. Thus, performances of trajectory tracking and disturbance suppression cannot be independently designed by PID control.

The DOB is an observer to estimate disturbances affecting a system [(7)]. Especially, the acceleration controller realized by the DOB is an effective control concept for motion control systems [(8)]. The acceleration controller realizes an ideal acceleration response suppressing disturbances. In addition, the acceleration controller can design performances of trajectory tracking and disturbance suppression independently. In DOB design, performance of disturbance suppression and order are determined by the Q-filter [(9)(10)]. According to the Q-filter, high-order DOBs have been studied by considering specific frequencies [(11)]. A periodic disturbance is usually compensated by high-order DOBs by ignoring high-frequency harmonics [(12)(13)]. In contrast to the high-order DOBs, an infinite-order disturbance observer (IFDOB) has been studied to suppress a periodic disturbance by considering all frequencies of the periodic disturbance [(14)]. However, the IFDOB is difficult to suppress low-frequency disturbances when the fundamental frequency is in the low-frequency domain. In this paper, the IFDOB is designed to suppress both the periodic disturbance and the low-frequency disturbances, and a designed IFDOB is proposed. The order of the dynamics is defined by the poles on the imaginary axis as

$$\begin{aligned} &\text{Zero} - \text{Order}: \ s = 0 \\ &\text{1st} - \text{Order}: \ s = 0,\ j\omega_1 \\ &\text{2nd} - \text{Order}: \ s = 0,\ j\omega_1,\ j\omega_2, \end{aligned}$$

where ω_1 and ω_2 are angular frequencies.

This paper is organized as follows: In Section 2, DOB design based on the internal principle and modeling of a periodic disturbance are described. Section 3 constructs and designs the IFDOB on the basis of the sensitivity and complementary sensitivity functions. Section 4 shows simulations. Finally, experiments using a multi-axis manipulator is shown in Section 5.

2. Design of a Disturbance Observer Based on the Internal Model Principle

2.1 Transformation of a Disturbance Observer

Disturbance suppression characteristic of a standard feedback system can be designed by the internal model principle. Block diagram of a DOB is transformed into the standard

* Department of System Design Engineering Keio University
3-14-1, Hiyoshi, Kohoku-ku, Yokohama 223-8522, Japan

© 2017 The Institute of Electrical Engineers of Japan.

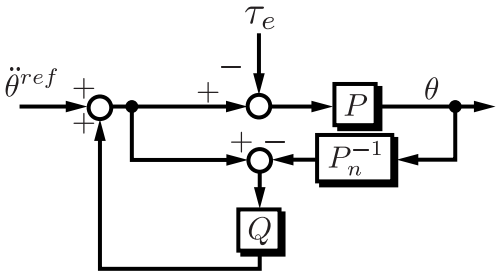

Fig. 1. Block diagram of a disturbance observer

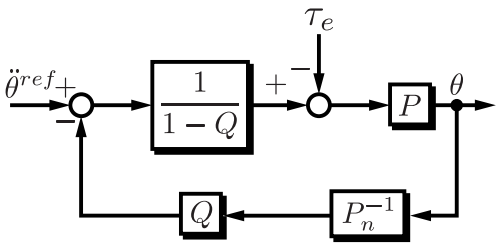

Fig. 2. Equivalent block diagram of Fig. 1

feedback system in this subsection. Figure 1 shows the block diagram of the DOB. τ_e, θ, P, Q, ^{ref}, $\dot{}$, $_n$, and $^{-1}$ denote the external disturbance, angle, plant, designed Q-filter, reference value, time differentiated value, nominal value, and inverse value, respectively. A controller of a feedback system must include dynamics of a disturbance in order to eliminate the disturbance on the basis of the internal model principle. The block diagram shown in Fig. 1 is transformed into Fig. 2 to consider the DOB as the standard feedback system. Thus, Fig. 2 shows the equivalent block diagram of the DOB. Then, $\frac{1}{1-Q}$ works as a controller of the standard feedback system. Therefore, disturbance suppression characteristic of a DOB is determined by designing $\frac{1}{1-Q}$ based on the internal model principle. Poles of the equivalent controller $\frac{1}{1-Q}$ including dynamics of a periodic disturbance is designed in Section 3.1.

2.2 Modeling of a Periodic Disturbance using Fourier Series Expansion A periodic disturbance is modeled to utilize for the controller design in this subsection. A periodic disturbance f_{dis} is expressed by Fourier series expansion as

$$f_{dis}(t) = \frac{a_0}{2} + \sum_{n=1}^{\infty} \left(a_n \cos(n\omega_0 t) + b_n \sin(n\omega_0 t)\right), \cdots\cdots \quad (1)$$

where a_0, a_n, and b_n denote the Fourier coefficients. ω_0 denotes the fundamental frequency. In order to obtain dynamics of the periodic disturbance, (1) is Laplace transformed into

$$\begin{aligned} F_{dis}(s) &= \mathcal{L}^{-1}\left[f_{dis}(t)\right] \\ &= \frac{1}{s}\frac{a_0}{2} + \sum_{n=1}^{\infty}\left(a_n \frac{s}{s^2+(n\omega_0)^2} + b_n \frac{n\omega_0}{s^2+(n\omega_0)^2}\right). \cdots\cdots \quad (2) \end{aligned}$$

The periodic disturbance includes an infinite number of poles as infinite-order dynamics, because, the denominator of (2) consists of s and $s^2 + (n\omega_0)^2$. Thus, the equivalent controller $\frac{1}{1-Q}$ of a DOB must include the infinite-order dynamics expressed as

$$s = jn\omega_0 \quad (n = 0, \pm 1, \pm 2, \ldots). \cdots\cdots\cdots\cdots\cdots\cdots \quad (3)$$

The poles that must be included to eliminate a periodic disturbance is thus obtained.

3. Design of an Infinite-Order Disturbance Observer

3.1 A Controller Based on the Internal Model principle The IFDOB that can compensate the periodic disturbance is designed in this subsection. (3) shows dynamics of the periodic disturbance. Thus, $\frac{1}{1-Q}$ is designed to include the poles as

$$\frac{1}{1-Q} = \frac{\gamma}{1-e^{-Ts}}, \cdots\cdots\cdots\cdots\cdots\cdots\cdots\cdots\cdots \quad (4)$$

where γ and T denote the design parameter and delay time, respectively. Then, the characteristic equation expressed as

$$1 - e^{-Ts} = 0 \cdots\cdots\cdots\cdots\cdots\cdots\cdots\cdots\cdots\cdots\cdots \quad (5)$$

includes the infinite number of poles. (5) can be transformed into

$$e^{j2n\pi} = e^{-Ts} \; (n = 0, \pm 1, , \pm 2, \ldots). \cdots\cdots\cdots\cdots\cdots \quad (6)$$

By eliminating the exponential, (6) is expressed as

$$-Ts = j2m\pi. \cdots\cdots\cdots\cdots\cdots\cdots\cdots\cdots\cdots\cdots\cdots \quad (7)$$

Thus, poles of (6) are obtained as

$$s = j\frac{2n\pi}{T} \; (n = 0, \pm 1, , \pm 2, \ldots). \cdots\cdots\cdots\cdots\cdots\cdots \quad (8)$$

From the above, the controller (4) includes an infinite number of poles. Since (3) and (8) are different, the delay time is determined as

$$T = \frac{2\pi}{\omega_0} \cdots\cdots\cdots\cdots\cdots\cdots\cdots\cdots\cdots\cdots\cdots\cdots\cdots \quad (9)$$

in order to match (8) with (3).

3.2 Designed Infinite-Order Disturbance Observer A designed IFDOB that suppresses both the low-frequency disturbances and the periodic disturbance is proposed in this subsection. The proposed method is constructed by designing γ included by the equivalent controller (4). γ of the designed IFDOB is determined as a PI controller multiplying $1 + \frac{g_{dis}}{s}$ and 2:

$$\gamma = 2\frac{s + g_{dis}}{s}, \cdots\cdots\cdots\cdots\cdots\cdots\cdots\cdots\cdots\cdots \quad (10)$$

where g_{dis} denotes the cutoff frequency. Thus, the proposed controller is expressed as

$$\frac{1}{1-Q(s)} = \frac{s+g_{dis}}{s}\frac{2}{1-e^{-Ts}}. \cdots\cdots\cdots\cdots\cdots\cdots \quad (11)$$

The designed Q-filter is derived form (11) as follows:

$$\begin{aligned} Q(s) &= 1 - \frac{s}{s+g_{dis}}\frac{1-e^{-Ts}}{2} \cdots\cdots\cdots\cdots\cdots\cdots \quad (12) \\ &= \frac{g_{dis}}{s+g_{dis}} + \frac{s}{s+g_{dis}}\frac{1+e^{-Ts}}{2}. \cdots\cdots\cdots\cdots \quad (13) \end{aligned}$$

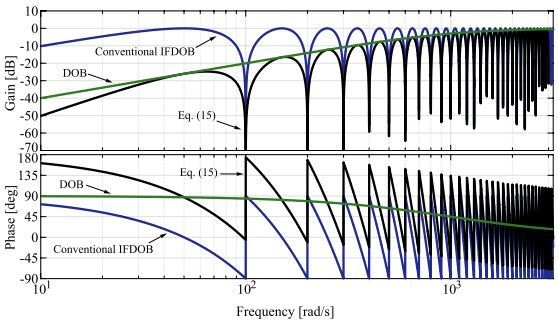

Fig. 3. Bode diagrams of sensitivity functions. The parameters are $\omega_0 = 100.0\,\mathrm{rad/s}$, $g_{dob} = 1000.0\,\mathrm{rad/s}$, $g_{con} = 1000.0\,\mathrm{rad/s}$, and $g_{dis} = 1000.0\,\mathrm{rad/s}$

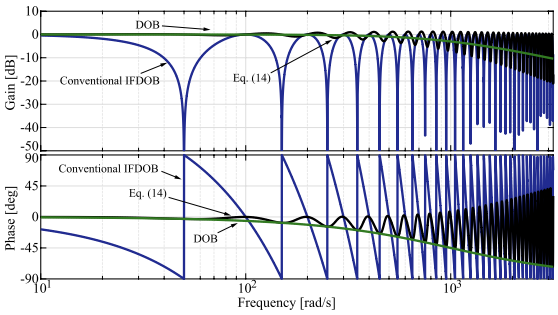

Fig. 4. Bode diagrams of complementary sensitivity functions. The parameters are $\omega_0 = 100.0\,\mathrm{rad/s}$, $g_{dob} = 1000.0\,\mathrm{rad/s}$, $g_{con} = 1000.0\,\mathrm{rad/s}$, and $g_{dis} = 1000.0\,\mathrm{rad/s}$

3.3 Sensitivity and Complementary Sensitivity Functions of the Designed Infinite-Order Disturbance Observer

This subsection describes sensitivity and complementary sensitivity functions of the designed IFDOB, because a sensitivity function indicates robustness against disturbances and a complementary sensitivity function indicates robust stability and noise sensitivity. Sensitivity and complementary sensitivity functions of the designed IFDOB are expressed as follows:

Sensitivity:

$$Q(s) = \frac{g_{dis}}{s + g_{dis}} + \frac{s}{s + g_{dis}} \frac{1 + e^{-Ts}}{2} \cdots\cdots\cdots\cdots (14)$$

Complementary sensitivity:

$$1 - Q(s) = \frac{s}{s + g_{dis}} \frac{1 - e^{-Ts}}{2} \cdots\cdots\cdots\cdots\cdots\cdots (15)$$

As the above, $1 - Q$ and Q are the sensitivity and complementary sensitivity functions in a DOB. Figures 3 and 4 show Bode diagrams of the sensitivity and the complementary sensitivity functions of the DOB and IFDOB. The DOB and the conventional IFDOB use the Q-filter expressed as follows:

DOB:

$$Q(s) = \frac{g_{dob}}{s + g_{dob}} \cdots\cdots\cdots\cdots\cdots\cdots\cdots\cdots\cdots (16)$$

Conventional IFDOB:

$$Q(s) = \frac{g_{con}}{s + g_{con}} \frac{1 + e^{-Ts}}{2}, \cdots\cdots\cdots\cdots\cdots\cdots\cdots (17)$$

where g_{dob} and g_{con} denote the cutoff frequencies of the DOB

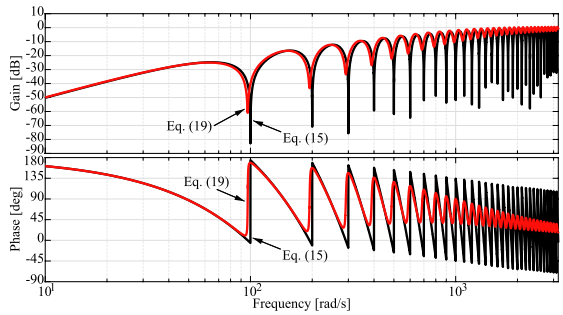

Fig. 5. Bode diagrams of sensitivity functions of the conventional and designed infinite-order disturbance observers. The parameters are $\omega_0 = 100.0\,\mathrm{rad/s}$, $g_{con} = 1000.0\,\mathrm{rad/s}$, $g_{dis} = 1000.0\,\mathrm{rad/s}$, and $g_t = 1000.0\,\mathrm{rad/s}$

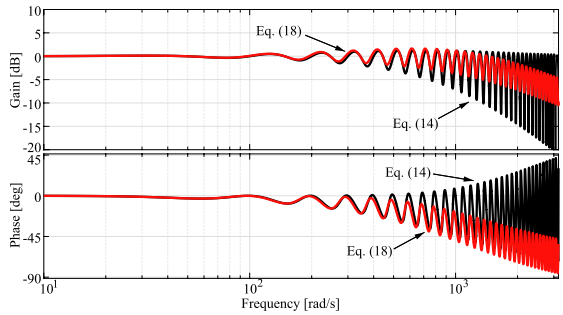

Fig. 6. Bode diagrams of complementary sensitivity functions of the conventional and designed infinite-order disturbance observers. The parameters are $\omega_0 = 100.0\,\mathrm{rad/s}$, $g_{con} = 1000.0\,\mathrm{rad/s}$, $g_{dis} = 1000.0\,\mathrm{rad/s}$, and $g_t = 1000.0\,\mathrm{rad/s}$

and the conventional IFDOB, respectively. The sensitivity and complementary sensitivity functions of the DOB (green line) show high-pass and low-pass characteristics. Hence, the DOB can suppress disturbances in the low-frequency domain However, it is difficult to suppress a periodic disturbance including harmonics. The conventional IFDOB (blue line) shows an infinite number of band-stop filters. Hence, the IFDOB can suppress a periodic disturbance, because it has the band-stop filters at frequencies of a periodic disturbance. However, the IFDOB whose ω_0 is at low-frequency domain is difficult to suppress disturbances in low-frequency domain. In contrast to the methods, the designed IFDOB whose design parameter γ is set as $2\frac{s+g_{dis}}{s}$ (black line) shows the combined characteristic of sensitivity function. The sensitivity function has both a low-pass characteristic and an infinite number of band-stop filters, and the complementary sensitivity function has an infinite number of weak band-stop filters. Therefore, the designed IFDOB realizes the best robustness to both low-frequency disturbances and a periodic disturbance, however, the complementary sensitivity function is the worst in the three methods.

3.4 Modification of the Designed Infinite-Order Disturbance Observer

The designed IFDOB $\gamma = 2\frac{s+g_{dis}}{s}$ is more robust than a DOB and the conventional IFDOB. However, noise sensitivity and robust stability are worsened by the tradeoff of sensitivity and complementary sensitivity functions. Thus, a low-pass filter is installed into (14) to modify balance of the tradeoff as follows:

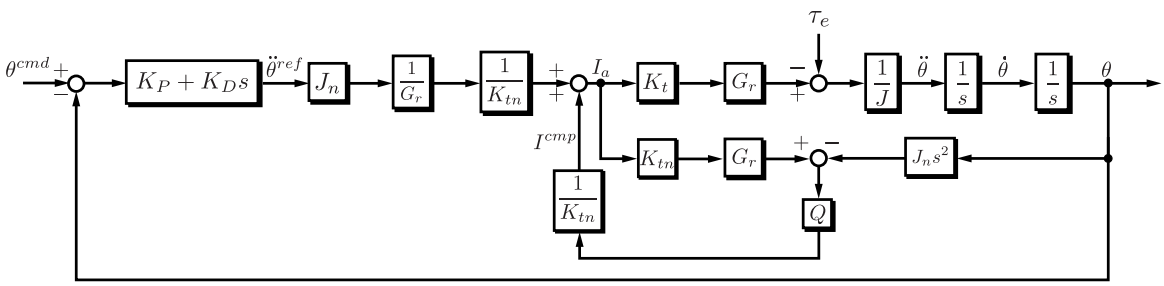

Fig. 7. Block diagram of the control system used by the simulations and the experiments

Table 1. Parameters of the simulations

Parameter	Description	Value
T_s	Sampling time	0.01 ms
T	Delay time	$\frac{2\pi}{\omega_0}$ s
J_n	Nominal inertia	0.0028 kgm^2
K_{tn}	Torque constant	1.18 Nm/A
G_r	Gear ratio	1
K_P	Proportional gain	400
K_D	Derivative gain	40
ω_0	Fundamental frequency	102 rad/s
g_{dob}	Cut-off freq.of the DOB	1000.0 rad/s
g_{con}	Cut-off freq.of the conventional FDOB	1000.0 rad/s
g_{dis}	Cut-off freq.of the designed IFDOB	1000.0 rad/s
g_t	Cut-off freq.of the designed IFDOB	1000.0 rad/s

Sensitivity:

$$Q(s) = \frac{g_{dis}}{s + g_{dis}} + \frac{g_t}{s + g_t}\frac{s}{s + g_{dis}}\frac{1 + e^{-Ts}}{2} \cdots\cdots (18)$$

Complementary sensitivity:

$$1 - Q(s) = \frac{s}{s + g_{dis}}\frac{s}{s + g_t} + \frac{s}{s + g_{dis}}\frac{g_t}{s + g_t}\frac{1 + e^{-Ts}}{2}, \cdots\cdots (19)$$

where g_t denotes the cutoff frequency. Figures 5 and 6 show the Bode diagrams of the sensitivity and complementary sensitivity functions of (14), (15), (18), and (19). The designed IFDOB is modified that the infinite number of band-stop filters of the sensitivity function is suppressed in the high-frequency domain, and the low-pass characteristic is added into the complementary sensitivity function. The designed IFDOB has enough robustness to both low-frequency disturbances and a periodic disturbance. In addition, robust stability of the designed IFDOB is ensured.

4. Simulations

The parameters used in the simulations are listed in Table 1. The block diagram of the control system is shown in Fig. 7, where K_P, K_D, J, G_r, K_t, ^{cmd}, I_a, and I^{cmp} denote the proportional gain, derivative gain, inertia, gear ratio, torque constant, command value, input current, and compensation current, respectively. The DOB, conventional IFDOB, and designed IFDOB use the Q-filter (16), (17) and (18), respectively. The command 0 was given, and the added disturbance is given as

$$\tau_e = \sin(10t) + \sum_{k=1}^{20} k \sin(k100t). \cdots\cdots\cdots\cdots\cdots\cdots (20)$$

The disturbance consists of the low-frequency sin wave and the periodic disturbance to confirm both robustness against the low-frequency disturbance and a periodic disturbance. Figures 8 and 9 show waveform of the simulation results and the added disturbance. The DOB and the designed IFDOB could suppress the low-frequency sin wave differently from the conventional IFDOB. Then, the designed IFDOB suppressed the periodic disturbance more than the DOB. Root mean square error and maximum angle error are calculated as shown in Table 2. In addition, discrete Fourier transform (DFT) results of the angle responses are shown in Fig. 10. In the frequency domain, the conventional IFDOB and the designed IFDOB suppressed the periodic disturbance. The DOB and the designed IFDOB suppressed the low-frequency disturbance. Thus, the best performance of root mean square

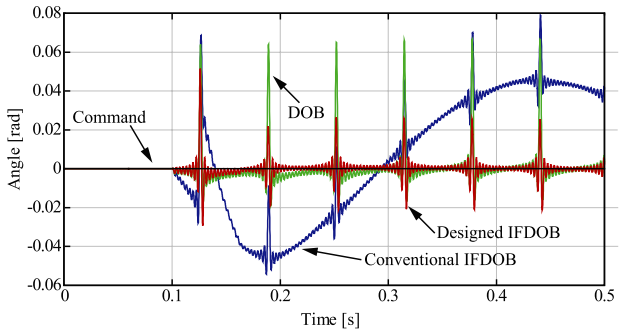

Fig. 8. Simulation results

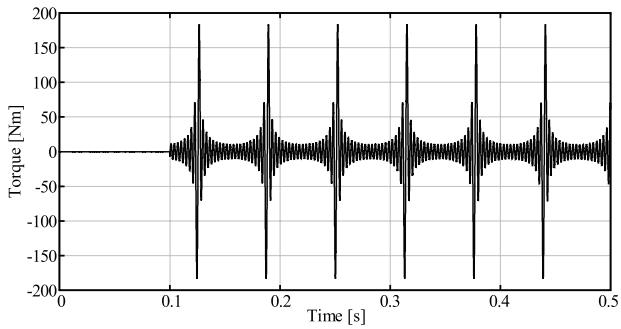

Fig. 9. Added disturbance

Table 2. Angle error analysis of the simulation results

Root mean square error	
DOB	9.18×10^{-3} rad
Conventional IFDOB	2.98×10^{-2} rad
Designed IFDOB	4.87×10^{-3} rad
Maximum angle error	
DOB	6.67×10^{-2} rad
Conventional IFDOB	7.92×10^{-2} rad
Designed IFDOB	5.17×10^{-2} rad

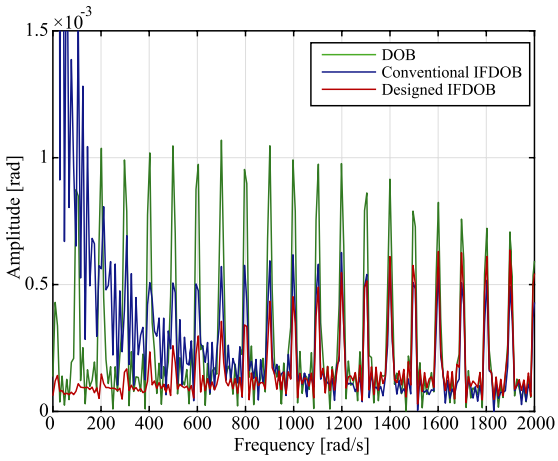

Fig. 10. DFT results of Fig. 8 from 0.1 s to 0.5 s

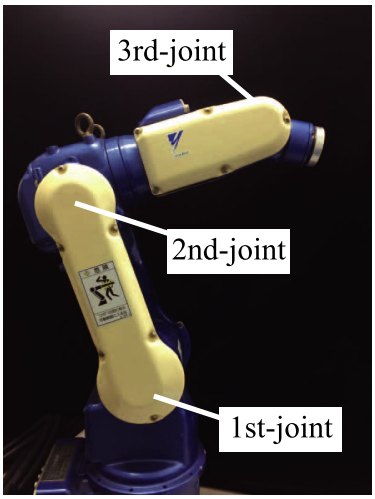

Fig. 11. Experimental system

Table 3. Parameters of the experiments

Parameter	Symbol	Value (1st, 2nd, 3rd) Joint
Sampling time	T_s	0.1 ms
Delay time	T_d	$\frac{2\pi}{\omega_0}$ s
Proportional gain	$\boldsymbol{K}_P$	(400, 400, 400)
Differential gain	$\boldsymbol{K}_D$	(40, 40, 40)
Motor inertia	$\boldsymbol{J}_n$	(7.0, 3.0, 0.3) kgm^2
Torque constant	$\boldsymbol{K}_{tn}$	(0.59, 0.59, 0.238) Nm/A
Gear ratio	$\boldsymbol{G}_r$	(192, 120, 80)
Length	$\boldsymbol{L}$	(0.26, 0.27, 0.09) m
Fundamental frequency	$\boldsymbol{\omega}_0$	(3.08, 3.08, 3.08) rad/s
Cutoff freq.of the DOB	$\boldsymbol{g}_{dob}$	(300, 300, 300) rad/s
Cutoff freq.of the conventional IFDOB	$\boldsymbol{g}_{con}$	(300, 300, 300) rad/s
Cutoff freq.of the designed IFDOB	$\boldsymbol{g}_{dis}$	(300, 300, 300) rad/s
Cutoff freq.of the designed IFDOB	$\boldsymbol{g}_t$	(300, 300, 300) rad/s

error and maximum angle error is achieved by the designed DOB as shown in Table 2. Validity of the designed IFDOB is confirmed.

5. Experiments

Experiments using a multi-axis manipulator were conducted. The experimental manipulator is shown in Fig. 11. The parameters used by the experiments are listed in Table 3. The PD gains and the cutoff frequencies were determined

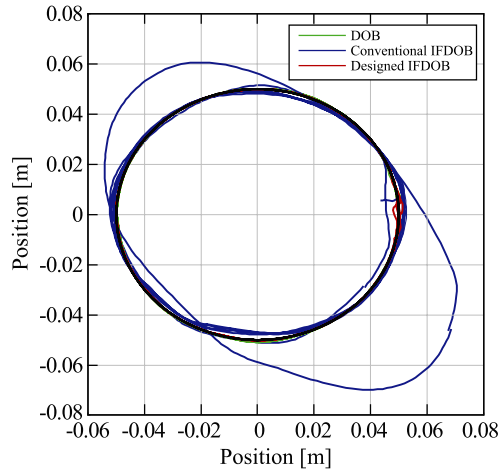

Fig. 12. Experimental results

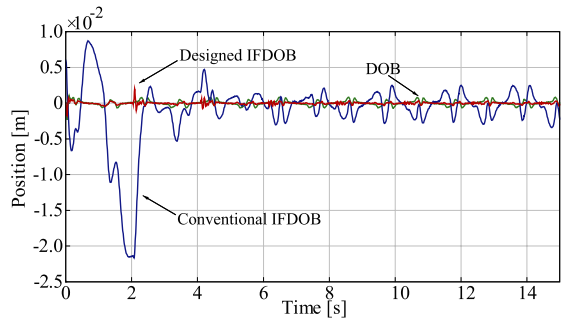

Fig. 13. Error of x-axis in Fig. 12

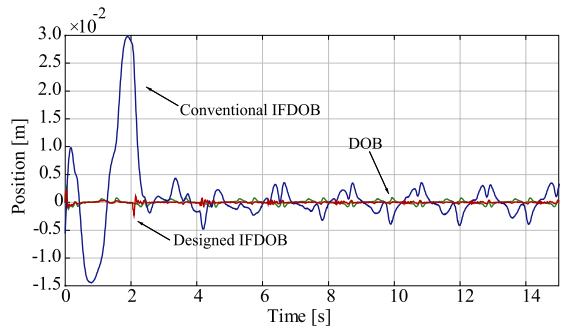

Fig. 14. Error of y-axis in Fig. 12

by considering the tradeoff, which is relation between sensitivity and complementary sensitivity functions. The control parameters are determined to satisfy enough stability, and the fundamental frequency was identified before the experiments. Block diagram of the control system is shown in Fig. 7. The DOB, conventional IFDOB, and designed IFDOB use the Q-filter (16), (17) and (18). The command of the work space is given as

$$x^{cmd} = x_0 - 0.05\cos(3t) \quad \cdots\cdots (21)$$

$$y^{cmd} = y_0 + 0.05\sin(3t), \quad \cdots\cdots (22)$$

where x, y, and $_0$ denote the x-axis value, y-axis value, and initial value, respectively. The command for the motors in joint space is calculated from (21) and (22). Figure 12 shows the whole experimental result. Figures 13, and

Table 4. Position error analysis of the experimental results

Root mean square error		
	X	Y
DOB	3.40×10^{-4} rad	3.59×10^{-4} rad
Conventional IFDOB	4.58×10^{-3} rad	6.18×10^{-3} rad
Designed IFDOB	1.89×10^{-4} rad	2.09×10^{-4} rad
Maximum position error		
	X	Y
DOB	2.33×10^{-3} rad	2.80×10^{-3} rad
Conventional IFDOB	2.17×10^{-2} rad	2.98×10^{-2} rad
Designed IFDOB	2.04×10^{-3} rad	2.45×10^{-3} rad

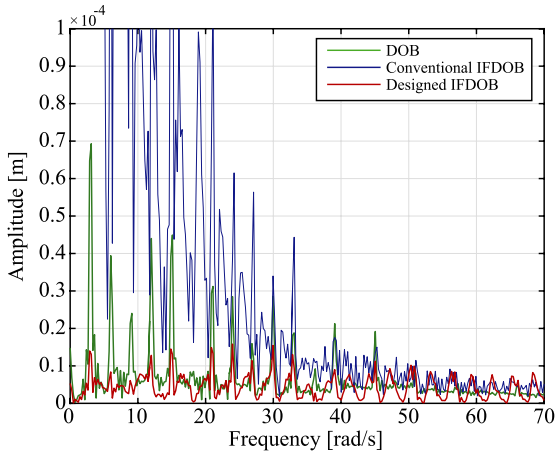

Fig. 15. DFT results of Fig. 13

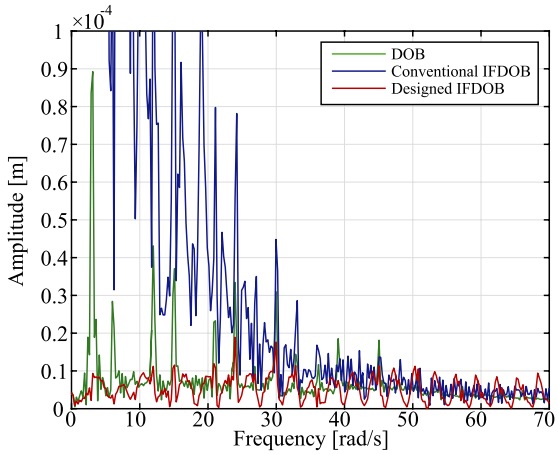

Fig. 16. DFT results of Fig. 14

14 show the errors of Fig. 12 in x-axis and y-axis. In addition, root mean square error and maximum position error are listed in Table 4. DFT results of Figs. 13 and 14 are shown in Figs. 15 and 16. Robustness to low-frequency disturbances and a periodic disturbance is confirmed in Figs. 15 and 16. The designed IFDOB suppressed both a periodic disturbance and low-frequency disturbances as shown in the analysis and the simulation results. Figures 3 and 5 show the sensitivity functions that indicate disturbance suppression characteristics, and Fig. 10 shows DFT results of the simulations. The experimental results show the same frequency characteristics as show in the figures. The conventional IFDOB (blue line) does not suppress the low-frequency disturbances, and DOB (green line) does not suppress the periodic disturbance enough. In contrast to them, the designed IFDOB (red line) achieves better suppression of both the low-frequency disturbances and a periodic disturbance.

6. Conclusion

This paper proposed a designed IFDOB which can suppress both a periodic disturbance and low-frequency disturbance. The proposed method was constructed by designing γ which is a design parameter of an IFDOB. The design is based on the sensitivity and complementary sensitivity functions. Robustness to disturbances including a periodic disturbance was improved. Practical validity was confirmed by the experiments using the multi-axis manipulator. As for a future work, the designed IFDOB will be applied to a resonant system in order to extend the scope of applications.

Acknowledgment

This research was partially supported by the Ministry of Internal Affairs and Communications, Strategic Information and Communications R&D Promotion Programme (SCOPE), 151203009, 2017.

References

(1) B. Francis and W. Wonham: "The internal model principle for linear multivariable regulators", *Applied Mathematics and Optimization*, Vol.2, No.2, pp.170–194 (1975)

(2) J. Han: "From PID to active disturbance rejection control", *IEEE Transactions on Industrial Electronics*, Vol.56, No.3, pp.900–906 (2009)

(3) K. Ohishi, K. Ohnishi, and K. Miyachi: "Torque-speed regulation of DC motor based on load torque estimation method", Proceedings of the IEEJ International Power Electronics Conference, IPEC, pp.1209–1218 (1983)

(4) W.-C. Gan and L. Qiu: "Torque and velocity ripple elimination of AC permanent magnet motor control systems using the internal model principle", *IEEE/ASME Transactions on Mechatronics*, Vol.9, No.2, pp.436–447 (2004)

(5) K.H. Ang, G. Chong, and Y. Li: "PID control system analysis, design, and technology", *IEEE Transactions on Control Systems Technology*, Vol.13, No.4, pp.559–576 (2005)

(6) C.-L. Lin, H.-Y. Jan, and N.-C. Shieh: "GA-based multiobjective PID control for a linear brushless DC motor", *IEEE/ASME Transactions on Mechatronics*, Vol.8, No.1, pp.56–65 (2003)

(7) K. Ohnishi, M. Shibata, and T. Murakami: "Motion control for advanced mechatronics", *IEEE/ASME Transactions on Mechatronics*, Vol.1, No.1, pp.56–67 (1996)

(8) E. Sariyildiz and K. Ohnishi: "Stability and robustness of disturbance-observer-based motion control systems", *IEEE Transactions on Industrial Electronics*, Vol.62, No.1, pp.414–422 (2015)

(9) F. Nishi and S. Katsura: "Nanoscale motion control using composite filter for disturbance observer", *IEEJ Transactions on Industry Applications*, Vol.4, No.2, pp.98–104 (2015)

(10) J. Su, W.-H. Chen, and B. Li: "High order disturbance observer design for linear and nonlinear systems", Proceedings of the IEEE International Conference on Information and Automation, ICIA, pp.1893–1898 (2015)

(11) T.T. Phuong, R. Furusawa, C. Mitsantisuk, and K. Ohishi: "Force sensing considering periodic disturbance suppression based on high order disturbance observer and kalman-filter", Proceedings of the International Conference on Human System Interactions, pp.336–341 (2011)

(12) K. Yamada, S. Komada, M. Ishida, and T. Hori: "Characteristics of servo system using high order disturbance observer", Proceedings of the IEEE Conference on Decision and Control, Vol.3, pp.3252–3257 (1996)

(13) J. Karttunen, S. Kallio, P. Peltoniemi, and P. Silventoinen: "Current harmonic compensation in dual three-phase pmsms using a disturbance observer", *IEEE Transactions on Industrial Electronics*, Vol.63, No.1, pp.583–594 (2016)

(14) H. Muramatsu and S. Katsura: "Periodic disturbance suppression based on infinite-order disturbance observer", Proceedings of the IEEJ International Workshop on Sensing, Actuation, and Motion Control, SAMCON, pp.2391–2404 (2016)

Hisayoshi Muramatsu (Student Member) received the B.E. degree in system design engineering from Keio University, Yokohama, Japan, in 2016. Since 2016, he has been in the Master's course at Keio University, Yokohama, Japan. His research interests include motion control and mechatronics. He is a Student Member of IEEJ, as well as a Student Member of the IEEE.

Seiichiro Katsura (Senior Member) received the B.E. degree in system design engineering and the M.E. and Ph.D. degrees in integrated design engineering from Keio University, Yokohama, Japan, in 2001, 2002 and 2004, respectively. From 2003 to 2005, he was a Research Fellow of the Japan Society for the Promotion of Science (JSPS). From 2005 to 2008, he was with Technology, Nagaoka, Japan. Since 2008, he has been with Keio University. His research interests include applied abstraction, human support, wave system, and systems energy conversion. Prof. Katsura serves as an Associate Editor of the IEEE Transactions on Industrial Electronics. He was the recipient of the IEEE Industrial Electronics Society Best Conference Paper Award in 2012 and JSPS Prize in 2016.